

RESEARCH ARTICLE

Macroalgae detritus decomposition and cross-shelf carbon export from shallow and deep reefs

Taylor Simpkins ,^{1*} Mirjam Van Der Mheen ,¹ Morten F. Pedersen ,² Albert Pessarrodona ,^{1,3,4}
Chari Pattiaratchi ,⁵ Thomas Wernberg ,^{1,2,6} Karen Filbee-Dexter ,^{1,6*}

¹UWA Oceans Institute & School of Plant Biology, The University of Western Australia, Perth, Western Australia, Australia; ²Department of Science and Environment, Roskilde University, Roskilde, Denmark; ³Conservation International, Arlington, Virginia, USA; ⁴International Blue Carbon Institute, Singapore; ⁵UWA Oceans Institute & Oceans Graduate School, The University of Western Australia, Perth, Western Australia, Australia; ⁶Flødevigen Research Station, The Institute of Marine Research, His, Norway

Abstract

Macroalgal forests have been suggested to export substantial amounts of carbon to deep ocean sinks and could account for 27–34% of annual blue carbon sequestered in Australia. However, a major knowledge gap concerns how carbon in the detrital tissue of the dominant seaweed species is remineralized as it is exported offshore. We quantified decomposition and carbon content in detrital tissue of dominant canopy-forming seaweeds *Ecklonia radiata* and *Scytothalia dorycarpa* at three depths (10, 20, and 50 m) in a 50 d in situ litterbag experiment in Western Australia. We then combined these rates with a particle tracking model to estimate the potential export of macroalgae detritus from our experiment sites into deeper waters. Decomposition of particulate organic carbon was fast relative to other cooler regions globally, and there were no significant differences between species and most depths. One-half of the detritus was remineralized within 12 (± 2) days for *E. radiata* and 8 (± 2) days for *S. dorycarpa*, with $\sim 8\%$ remaining for both species after 50 d in situ. Based on simulated transport times and decomposition, 10% and 11% of the *E. radiata* and *S. dorycarpa* detritus from shallow reefs (10–20 m) were exported beyond the shelf break (≥ 200 m) whereas 47% and 37% were exported from deep reefs (50 m). These estimates highlight the variable but substantial carbon sequestration potential across the coastal zone.

Anthropogenic greenhouse gas emissions over the past century have caused an unprecedented level of warming (1.0°C) that is driving significant ecological and socioeconomic decline globally (Stephen 2021). While commitments to emissions reductions will substantially reduce warming, global

temperature is not projected to stabilize under the targeted 2.0°C by the end of the century with these changes alone. Consequently, there is an urgent need to investigate additional greenhouse gas emission mitigation strategies such as the safeguarding of both terrestrial and marine vegetated ecosystems that naturally draw down atmospheric carbon.

The management and restoration of blue carbon (carbon stored and sequestered by coastal vegetated ecosystems) is an emerging nature-based solution to mitigate climate change (Pidgeon 2021; Vanderklift et al. 2022). The world's coastal mangroves, salt marshes, and seagrass meadows collectively store and sequester 0.5–0.8% of anthropogenic carbon dioxide emissions (141–466 tons of carbon yr⁻¹) (Macreadie et al. 2021). Macroalgal forests are not included in these blue carbon estimates, yet emerging evidence suggests they may also be responsible for substantial amounts of carbon sequestration through: the export of particulate (POC) and dissolved organic

*Correspondence: taylor.simpkins@research.uwa.edu.au; kfilbeedexter@gmail.com

This is an open access article under the terms of the [Creative Commons Attribution-NonCommercial](https://creativecommons.org/licenses/by-nc/4.0/) License, which permits use, distribution and reproduction in any medium, provided the original work is properly cited and is not used for commercial purposes.

Associate editor: Anna Armitage

Data Availability Statement: The data that support the findings of this study are openly available in GitHub at <https://github.com/T-Simpkins/macroalgae-decomposition>, and available upon request with the corresponding author.

carbon to deep ocean water bodies with long ventilation times, the burial of detrital carbon in marine sediments, as well as the production of refractory dissolved organic carbon (Krause-Jensen and Duarte 2016; Ortega et al. 2019; Filbee-Dexter et al. 2024; Pessarrodona et al. 2023; Queiros et al. 2023). First-order estimates of particulate macroalgal organic carbon sequestration suggest a contribution of 56 (10–170) tons of carbon yr^{-1} globally, which represents a sizeable fraction ($\sim 49\%$) of the total sequestration potential of coastal vegetated ecosystems (Filbee-Dexter et al. 2024). However, there remains considerable uncertainty in a critical step of carbon sequestration: The pathways of carbon transport to deep ocean water bodies, which are influenced by local and regional-scale oceanographic processes (Broch et al. 2022; Hurd et al. 2022; Queiros et al. 2023; van der Mheen et al. 2024) and biological processes (Filbee-Dexter et al. 2022; Wright et al. 2022; Queiros et al. 2023). Specifically, in situ measures of remineralization and offshore transport of macroalgal carbon are lacking in many regions and should be accounted for to better understand how macroalgal forests influence marine carbon cycling and to improve the accuracy of global macroalgal carbon sequestration estimates (Macreadie et al. 2019; Pessarrodona et al. 2023).

The production of detritus drives the flux of macroalgal carbon that leaves donor reefs in the form of POC. Macroalgal forests are highly productive ecosystems (Pessarrodona et al. 2022) and, on average, 82% of macroalgal net primary production is released as detritus, which is either consumed and integrated into the food web or buried and stored in marine sediments (Krumhansl and Scheibling 2012). Macroalgal detritus, POC, is estimated to comprise approximately half of the carbon exported to sinks (43% of net primary production), the other half being dissolved organic and inorganic carbon, yet the fate of dissolved organic carbon is not as well understood as that of POC and may be overestimated (Krause-Jensen and Duarte 2016; Paine et al. 2021). Generally, macroalgal POC is produced through erosion (the continuous senescence of tissue at the distal region of the blade) and dislodgement (the detachment of entire thalli or old blades) and the proportion of detritus produced through either blade erosion or dislodgement is variable with species (Krumhansl and Scheibling 2012; de Bettignies et al. 2013; Pedersen et al. 2019). For example, in Australia, *Ecklonia radiata* releases the majority of annual detrital production through distal lateral erosion with an autumn flux (~ 5 g fresh weight [FW] individual $^{-1}$ d $^{-1}$) at least twice as high as in all other seasons (de Bettignies et al. 2013), but in northern Norway, *Laminaria hyperborea* releases the majority of detritus in its annual cast of old blades and dislodgement, with only one quarter of detrital production generated by distal erosion (Pedersen et al. 2019). Pulses of macroalgal detrital production in autumn and winter have been attributed to seasonally declining tissue quality and increasing frequency of storms (Krumhansl and Scheibling 2012; de Bettignies et al. 2013; Pedersen et al. 2019). Once

produced, the fate of detrital carbon is intrinsically linked to a range of ocean transport and mixing processes that expose the detritus to different environmental conditions and microbial and detritivore communities (Zarco-Perello et al. 2019; Queiros et al. 2023). Understanding the transfer of macroalgal carbon from donor reefs to recipient habitats therefore requires knowledge of both oceanographic processes and detrital decomposition, which can be resolved using particle tracking models (Filbee-Dexter et al. 2020; Broch et al. 2022; Queiros et al. 2023).

In the marine environment, detritus can be transported tens to hundreds of kilometers from source reefs, where it can contribute to POC in littoral food webs, in beach wrack, in the deep ocean, or become buried in shelf sediments (Hansen 1984; Pedersen et al. 2019; Broch et al. 2022). Oceanographic and topographic features such as submarine canyons (Vetter and Dayton 1998; Macreadie et al. 2019) and cross-shelf currents known as Dense Shelf Water Transport (DSWT) can facilitate and potentially expedite the export of POC offshore beyond the shelf break to the deep ocean (Pattiaratchi et al. 2011; van der Mheen et al. 2024). The DSWT occurs when evaporative or cooling processes increase the density of sea water near the coast, which sinks and flows offshore along the sea bed, transporting coastal detritus within the bottom layers of this dense water mass (Pattiaratchi et al. 2011; Mahjabin et al. 2019; van der Mheen et al. 2024). The DSWT has been documented in over 60 locations globally (Ivanov et al. 2004) and along the $> 10,000$ km of Australian coastline (Mahjabin et al. 2020). Submarine canyons have also been identified as important channels for the export of POC from coastal habitats to the deep sea (Vetter and Dayton 1998). Despite widespread evidence of macroalgal detritus in the deep sea—occurring in reservoirs up to 4000 m deep and 5000 km offshore, and in the gut content of abyssal isopods sampled at 6475 m (Wolff 1962; Ortega et al. 2019)—few studies have quantified rates of export to these sinks.

The transformation (decomposition rate) of macroalgal detritus as it is transported away from donor reefs is a strong determinant of how much POC can reach sink habitats, with slower decomposition increasing the possibility of macroalgal carbon sequestration. Decomposition of detritus specifically refers to processes that remove carbon from the detrital pool, such as leaching of nutrients, microbial breakdown, and consumption by detritivores, ultimately affecting the amount of total carbon available for sequestration through burial of detritus in shelf sediments or export to deep ocean water bodies (Kristensen 1994). Detritus travels through environments with varying biochemical and physical conditions (e.g., light, temperature, and current velocity), which affect the rate of decay (Pedersen et al. 2021). Macroalgal decomposition has been studied both in situ, to capture the local effects of microbial decay, grazing and seasonality, and in controlled mesocosm experiments, to quantify the effects of light, temperature, and oxygen conditions (Kirschbaum 2010; de Bettignies

et al. 2020; Pedersen et al. 2021). Decomposition of macroalgal detritus generally follows a negative exponential decay model (Kristensen 1994). The presence of light may slow down decay as algal detritus can continue to gain biomass through photosynthesis for some time (de Bettignies et al. 2020; Frontier et al. 2021; Wright et al. 2022). Macroalgal decomposition rate is positively correlated to temperature (Pedersen and Johnsen 2017; Filbee-Dexter et al. 2022), but seasonal changes in temperature can have little effect on decomposition rate if the environment has a narrow and low temperature range (Pedersen et al. 2021). Fauna associated with decomposing detritus can play a substantial role in breaking down and remineralizing macroalgal POC (Robertson and Lucas 1983) and often increase decomposition rate (Filbee-Dexter et al. 2020), but in some cases (e.g., Amphipoda) they can slow overall decomposition through their selective consumption of decaying tissue, which prevents tissue disintegration by microbes (Bedford and Moore 1984). Anoxic conditions may also slow the rate and extent to which macroalgal detritus is decomposed (Pedersen et al. 2021). Decomposition rate can also vary among macroalgal species, with fast-growing macroalgae, such as *Ulva*, *Ceramium*, *Polysiphonia*, and *Gracilaria* having typically faster decay rates (-3.2% to $-25.6\% \text{ d}^{-1}$; e.g., Banta et al. 2004; Pedersen and Johnsen 2017) than more slow-growing macroalgae belonging to Laminariales and Fucales (-0.7% to $-8.3\% \text{ d}^{-1}$) (Smith and Foreman 1984; de Bettignies et al. 2020). Under certain conditions, the refractory fractions of macroalgal detritus may take hundreds of days to years to decay and could play an important role in the refractory blue carbon pathway (Pedersen et al. 2021; Trevathan-Tackett et al. 2015). Despite the importance of decomposition rate in determining the fate of macroalgal carbon, the decomposition rates for *E. radiata* and *S. dorycarpa*—two of the dominant habitat-forming temperate seaweeds along Australia's Great Southern Reef (Martinez et al. 2018)—have not been quantified in situ, which is a major knowledge gap and challenges estimates of macroalgal blue carbon sequestration in this area.

Our study investigates the extensive macroalgal forests along the southern coast of Australia collectively referred to as the Great Southern Reef (Coleman and Wernberg 2017; Wernberg 2019), which contributes a greater net economic benefit ($\$22.8 \pm 3.8\text{bn US\$ yr}^{-1}$) from blue carbon storage and sequestration than any country on the planet (Bertram et al. 2021). It is estimated that Australian macroalgal forests export more POC to deep ocean sinks than any other country worldwide (1.3–26.2 million tons of carbon yr^{-1}) (Filbee-Dexter et al. 2024), and the macroalgal forests in the Great Southern Reef contribute as much as 30% (27–34%) of all blue carbon in Australia (Filbee-Dexter and Wernberg 2020). *Ecklonia radiata* and *S. dorycarpa* are the dominant kelp and furoid species on the Great Southern Reef, Australia, found along 6000 and 3000 km of Australia's coastline, respectively (Coleman and Wernberg 2017; Wernberg 2019). While *E.*

radiata is found in Australia, New Zealand, and South Africa, *S. dorycarpa* is endemic to Australia (Wormersley 1987; Wernberg et al. 2003; Coleman and Wernberg 2017). Decomposition of *E. radiata* detritus has been studied in Western Australia in the surf zone (30–40 d turnover) and in beach wrack (21 d turnover) (Hansen 1984), but not in subtidal shelf environments. Little is known about how physical and biological processes transform particulate detritus from *S. dorycarpa* and *E. radiata* as it is exported offshore, and quantifying the decomposition of macroalgal detritus on the continental shelf is a key unknown in Australian blue carbon research.

In this study, we used an in situ litter bag experiment to (1) quantify decomposition rates of dominant kelp (*E. radiata*) and furoid (*S. dorycarpa*) detritus; and (2) assess whether decomposition of macroalgal detritus was affected by changing environmental factors (temperature, light, and meiofauna) along the depth gradient of the continental shelf. We then used these decomposition rates in a particle tracking simulations to estimate the export rate of macroalgal detritus beyond the continental shelf and into the deep ocean ($>200\text{-m}$ depth). This knowledge is essential to understand the potential role of Australia's Great Southern Reef in marine carbon sequestration.

Materials and methods

Study area

This study was conducted on the Rottneest Continental Shelf in Southwest Australia (Fig. 1a). The Rottneest Continental Shelf gradually slopes to 50 m then drops sharply to the continental shelf edge at 200 m (Fig. 1b), which is also the depth to which the dominant surface current (Leeuwin Current) exists (van der Mheen et al. 2024). Cross-shelf currents (DSWT) form in austral winter and can be responsible for transporting particulate organic matter from the coast to the edge of the continental shelf (Pattiaratchi et al. 2011; van der Mheen et al. 2024). Macroalgal reefs are distributed along the inner shelf and outer shelf, with outer shelf reefs estimated to comprise one third of total macroalgal reefs from 0 to 60 m (Bellchambers 2017).

Sample collection

Live *E. radiata* and *S. dorycarpa* thalli were collected on May 30, 2021 from “3 Mile Reef” in Marmion Marine Park, Western Australia (31.789367°S, 115.679017°E). The algae were kept cool and transported in wet calico bags to the Indian Ocean Marine Research Center at Waterman's Bay, Western Australia, and stored in a 10°C cool room for 72 h before being used in the experiment. Individual samples of *E. radiata* and *S. dorycarpa* were spun dry, cut along the lamina–lateral interface (approximately 5–10 cm above the meristem), trimmed to a FW of 20 g and placed in flexible litter bags (“onion bags”, mesh-size = 5 mm, $\sim 200 \text{ cm}^3$) made of polypropylene. Fourteen litterbags (seven of each species) were then combined

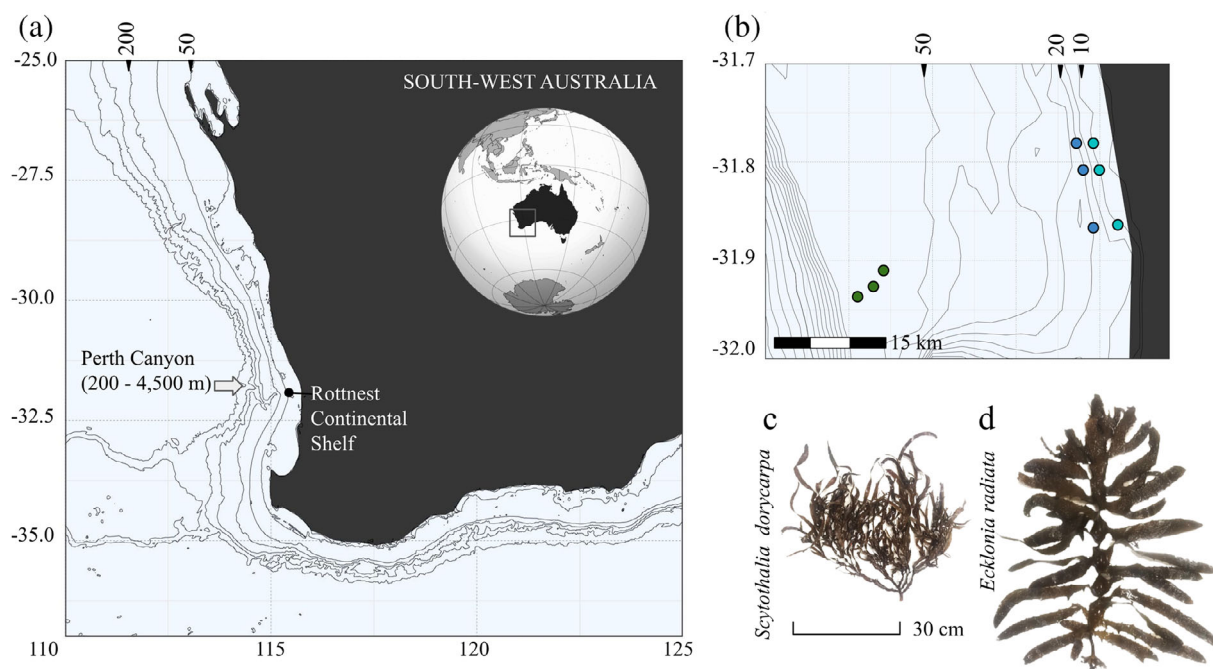


Fig. 1. Site map of the in situ decomposition experiment. **(a)** Location of the Rottneest Continental Shelf in respect to the southwest region of Australia, with a 200-m contour representing the continental shelf edge and head of the Perth Canyon. **(b)** Coordinates of each litterbag array, with colors representing the depth of each coordinate (teal = 10 m, blue = 20 m, and green = 50 m), and isobaths (m) represented at the top of each map. **(c)** *Scytothalia dorycarpa* specimen. **(d)** *Ecklonia radiata* specimen. Maps generated in R using the “ggspatial” package with National Oceanic and Atmospheric Administration’s bathymetry data in the “marmap” package.

into larger (17 cm diameter, 3900 cm³, mesh size = 8 mm × 10 mm) rigid litterbags to simulate in situ accumulations of detritus. A total of 45 large litterbags containing 630 individual flexible bags were then randomized and assigned to an array for each site.

Experimental design

In-situ decomposition of *E. radiata* and *S. dorycarpa* was measured in a 50 d litterbag experiment at nine sites and three depths (three sites per depth; 10, 20, and 50 m) across the Rottneest Continental Shelf, Western Australia (Fig. 1). Depth treatments replicated varying physical conditions (e.g., light, temperature, and current velocity) that macroalgal detritus travels through while exported across the shelf. The litterbags were deployed between May and July 2021 to coincide with the timing of the natural peak in detrital production of the two algal species. Rigid litterbags (five per site) were secured to the bottom with a 1-m chain attached to a 25-kg concrete mooring block. Each mooring was equipped with a HOBO Pendant® G Data Logger UA-004-64 (water velocity) and a HOBO Pendant® Temperature/Light Data Logger—UA-002-064 (accuracy: 0.47°C and resolution: 0.1°C at 25°C) to record abiotic conditions every 15 min (June 2–16, 2021) at each site. Mooring blocks were lowered to the seafloor from the surface using a 12-mm polyethylene line and marked with a surface

float. One rigid litterbag (containing seven flexible bags of each species) per time point was retrieved from each of the nine locations (three per depth treatment) after 14, 31, and 50 d. Deep (50 m) moorings could not be located during sampling time points T2 (31 d) and T3 (50 d), likely due to ship traffic in the area cutting the lines. Following retrieval, litterbags were transferred to the Waterman’s Bay facilities in a cooler on ice and carefully rinsed in freshwater to remove sediment and fauna. The macroalgal remains were weighed (FW) and then immediately dried at 60°C for 48 h to constant weight. Dried macroalgal materials were weighed to determine the dry weight (DW). Colonizing fauna were removed from macroalgae, weighed (FW) and frozen.

Chemical analysis

Dried samples were homogenized to a fine powder using a ball mill, and 5 µg subsamples were analyzed for C and N using a continuous flow system consisting of a Delta V Plus mass spectrometer connected to an elemental analyzer Thermo Flush 1112 via ConFlo IV (Thermo-Finnigan/Germany) in the West Australian Biogeochemistry Center, The University of Western Australia. Standards NBS22, IAEA603, USGS24, and USGS40 were used for normalization of C, and USGS40, IAEA N1, IAEA N2, and USGS32 for N (Skrzypek 2013).

Particle tracking model

We ran hydrodynamic and particle tracking simulations to illustrate the potential transport of macroalgal detritus from our litterbag experiment sites into the deep sea. These simulations used the same hydrodynamic and particle tracking model, particle “behavior” assumptions, and ocean current forcing as the simulations in van der Mheen et al. (2024), which considered the total export potential of macroalgal detritus from the wider Rottneest Continental Shelf region. For convenience, we summarize the main points here.

The software Opendrift-v1 (Dagestad et al. 2018) was used to run Lagrangian particle tracking simulations to determine the transport of macroalgal detritus from all litterbag sites. We released 500 particles daily at midnight from each of the litterbag sites from the 1st of January until the 31st of December and continued the simulation until the 31st of January the following year. From the simulation, we recorded the percentage of particles exported beyond the continental shelf. We use a threshold depth of 200 m, where mixing of water with the surface is unlikely to occur since 200 m is the depth of the continental shelf edge and the depth to which the dominant surface current (Leeuwin Current) extends (van der Mheen et al. 2024). In this study, particles that pass below this depth threshold are considered exported to the deep ocean, while particles exported to depths shallower than 200 m are considered to be retained on the shelf and either remineralized, grazed, buried in the shelf, or washed ashore as beach cast. We note that the focus of our model is to examine the offshore export of negatively buoyant detritus in DSWT along the seabed, and we therefore do not include wave or wind forcing. This region is a microtidal region, with a tidal range of only ~ 0.5 m (Pattiaratchi et al. 2011), so we do not expect the release time in relation to the tidal cycle to influence particle tracking simulation results. We ran the simulation for the year 2017, which can be considered a “typical” year along the west coast of Australia because there were both neutral El Niño Southern Oscillation (Wolter and Timlin 2011) and Indian Ocean Dipole (Yamagata et al. 1999) conditions during this year. We used a timestep of 10 min and output particle locations every 3 h.

The particle tracking simulations were forced by ocean currents in the bottom layer (considering *E. radiata* and *S. dorycarpa* are both negatively buoyant and are transported along the seafloor) from a regional ocean model, Central Western Australia-Regional Ocean Modeling System (CWA-ROMS), which is a high-resolution realistic setup of the ROMS and was run in hindcast mode for this study. Output from the CWA-ROMS model is available at a 3-hourly temporal resolution, approximately 2 km (1.7–2.1 km) horizontal resolution on the continental shelf, and in 25 vertical layers (of which we used the bottom layer). Because CWA-ROMS uses terrain-following sigma-layers, the height of the bottom layer above the seafloor varies between less than 1 m and up to 10 m on the Rottneest Continental Shelf, to a maximum of 260 m in the deeper

ocean past the continental shelf. Information on forcing and boundary conditions used in CWA-ROMS is given in van der Mheen et al. (2024). Model forcing included water level variations (tides and non-tidal changes) and a full suite of meteorological data (winds and air–sea fluxes). Mahjabin et al. (2019) validated a model nested within CWA-ROMS, which accurately reproduces DSWT, and van der Mheen et al. (2024) also illustrated DSWT in the larger (non-nested) CWA-ROMS model.

Following van der Mheen et al. (2024), we let particles drift passively with bottom ocean currents. This is justified by sensitivity analyses in van der Mheen et al. (2024) that showed that the sensitivity to including a threshold velocity for small and medium-sized *E. radiata* particles in simulations was minimal. They also showed that correcting for a logarithmic vertical current profile in the bottom layer had minimal influence on the results.

Estimates of percent POC export to 200-m depth or more were calculated by multiplying the percent of particles exported to > 200 m (d^{-1}) with the proportion of initial POC remaining (d^{-1}) from days 0 to 60, then compiling all 61 daily estimates. Daily estimates of the proportion of initial POC remaining were calculated using an exponential decay model derived from the percent carbon content of all samples in our litterbag experiment.

Statistical analysis

Detritus decomposition rates were estimated using an exponential decay model. A nonlinear least squares regression (nls()) function in R package “stats”) was used to analyze remaining biomass and remaining carbon measurements over four time points approximately 2 weeks apart for each species and depth treatment. The exponential decay model was sequentially improved by adding species-specific γ -intercepts and refractory fractions, and goodness of fit was validated with Akaike information criterion (AIC) values (Supporting Information Table S1).

$$A(t) = I \times (A_0 \times e^{kt}) + R_G$$

where $A(t)$ is the remaining biomass at time t (days), I is the γ -intercept, A_0 is the initial biomass at time zero, k is the decay rate constant, and R_G is the refractory fraction (value below the asymptote). R_G was only included when significantly greater than zero. Heteroscedasticity of sample variance in the data was normalized by weighting time in a generalized model using nonlinear least squares.

Statistical differences in decomposition rate and chemical content of detrital tissue were analyzed using ANOVA to compare treatment variance in multiple response variables (percent remaining biomass, percent remaining carbon, percent C, percent N, and C : N ratio) with explanatory variables (time, species, and depth) as fixed factors. Assumptions of normality and homogeneity of variance were tested by plotting

residual variance and frequency. Post hoc Tukey HSD tests were used to test for significance among species, depth, and time treatments.

Results

Environmental parameters

Water temperature (mean \pm 1 SD) at experimental sites was $20.2 \pm 0.7^\circ\text{C}$ (range: $18.3\text{--}21.9^\circ\text{C}$) at 10 m, $20.3 \pm 0.7^\circ\text{C}$ ($18.6\text{--}21.9^\circ\text{C}$) at 20 m, and $21.6 \pm 0.7^\circ\text{C}$ ($20.6\text{--}23.1^\circ\text{C}$) at 50 m (Supporting Information Table S2). Light exposure (mean \pm SE) was higher and more variable at 10 m sites (39 ± 6 lux) than at 20 m sites (11 ± 2 lux), while no light was detected by loggers at 50-m sites. Video surveys conducted on July 3, 2022, at 11:00 a.m. looking for the lost 50-m bags, provided observational evidence of light reaching the bottom at all the 50-m sites, although light intensity was lower than at the shallow sites (Fig. 4b). Meiofauna (1–5 mm) were observed on the tissue of both species (predominantly amphipods around decaying tissue) across all depths, but fresh biomass at 20-m depth sites was substantially greater (over tenfold) than at 10- and 50-m depth sites (Supporting Information Table S3).

Interspecific variation in decomposition

Overall, there were no significant differences between the decomposition rate (k) of *S. dorycarpa* and *E. radiata* in this region ($p = 0.101$; Table 1, Fig. 2; Supporting Information Table S4). However, the decomposition of *S. dorycarpa* detritus at 20 m occurred significantly faster than at 10 m ($p = 0.003$; Table 1; Supporting Information Tables S4, S5). Although the decomposition rate was not significantly different between species, after 2 weeks in situ, *E. radiata* tissue

($40.7\% \pm 4.1\%$ SE) had 1.7 times more of the initial carbon remaining compared to *S. dorycarpa* ($26.7\% \pm 1.7\%$ SE) ($p < 0.001$) (Fig. 2). The decomposition of detrital tissue in both species across all depths fitted a negative exponential model. Percent remaining biomass after 2 weeks (rb_{14}) was more variable in *E. radiata* ($rb_{14} = 0\text{--}125\%$, SD = 29.6%, SE = 4.1%) than in *S. dorycarpa* ($rb_{14} = 6\text{--}83\%$, SD = 12.6%, SE = 1.7%) (Fig. 2; Supporting Information Table S5). The refractory fraction of detrital tissue was significantly different from zero for *S. dorycarpa* ($8.5\% \pm 1.5\%$ SE) ($t = 5.710$; $p < 0.001$), but not for *E. radiata* ($8.0\% \pm 6.1\%$ SE) ($t = 1.308$; $p = 0.193$) (Table 1). Reported means for the refractory fraction did not differ significantly between species ($t_{\text{species}} = 0.073$, $p = 0.942$).

Depth effect on decomposition

Depth had a significant effect on the decomposition rate of *S. dorycarpa* ($F_{\text{depth}} = 6.284$; $p = 0.003$), but not *E. radiata* ($F_{\text{depth}} = 1.843$; $p = 0.165$), with the decomposition of *S. dorycarpa* at 20 m sites being 66% and 65% slower than at 10 and 50 m sites, respectively (Table 1).

Chemical content of decomposing detritus

Carbon and nitrogen content did not vary with depth treatment for either *E. radiata* (%C: $t_{\text{depth}} = 0.918$; $p = 0.362$; %N: $t_{\text{depth}} = 0.237$; $p = 0.813$) or *S. dorycarpa* (%C: $t_{\text{depth}} = 1.165$; $p = 0.247$; %N: $t_{\text{depth}} = -0.796$; $p = 0.428$) (Fig. 3; Supporting Information Table S6). The initial carbon content of *E. radiata* and *S. dorycarpa* did not differ significantly ($t_{\text{species}} = -1.167$; $p = 0.245$; Fig. 3). However, the carbon content of *E. radiata* decreased by $\sim 7\text{--}8\%$ over the course of the experiment ($t_{\text{time}} = -2.547$; $p = 0.012$; Fig. 3; Supporting Information Tables S6, S7), whereas the carbon content of *S. dorycarpa* remained constant throughout the experiment ($t_{\text{time}} = 0.294$;

Table 1. Negative exponential decay estimates (k) (based on changes in C-mass over time) and residual biomass (R_G) with two fixed factors (species and depth) and 95% confidence intervals. Negative exponential decay equation: $A(t) = I \times (A_0 \times e^{kt}) + R_G$. Half-life = $\ln(0.50)/k$. Asterisks show significantly different k values from other depth treatments within species (Supporting Information Table S4d).

Treatment	k (Parameter estimate)	[Lower–upper 95% CI]	Half-life (days)
<i>Ecklonia radiata</i>			
10 m	−0.077	[−0.104 to −0.051]	9.00
20 m	−0.049	[−0.058 to −0.040]	14.15
50 m	−0.053	[−0.077 to −0.029]	13.08
Mean (10–50 m)	−0.060	[−0.106 to −0.045]	12.08
<i>Scytothalia dorycarpa</i>			
10 m	−0.103	[−0.114 to −0.080]	6.73
20 m	−0.068*	[−0.077 to −0.061]	10.19
50 m	−0.105	[−0.117 to −0.093]	6.60
Mean (10–50 m)	−0.092	[−0.138 to −0.097]	7.84
Species	R_G (mean \pm SE)	t (R_G)	p (R_G)
<i>Ecklonia radiata</i>	8.0 ± 6.1	1.308	0.1929
<i>Scytothalia dorycarpa</i>	8.5 ± 1.5	5.710	<0.001

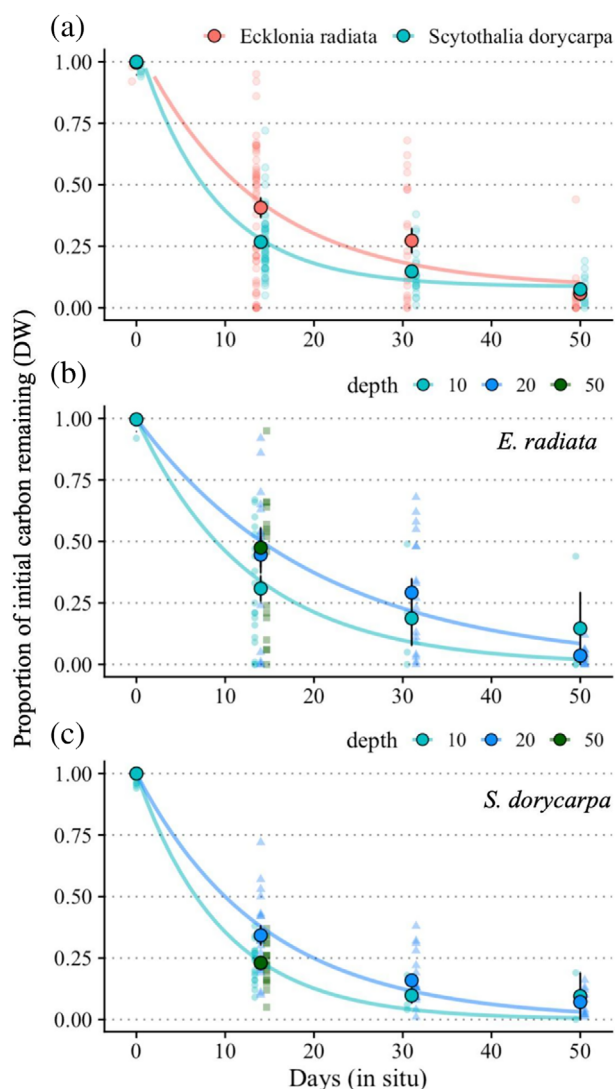


Fig. 2. Changes in the carbon (C) biomass of macroalgae detritus over time. Solid circles represent the mean (± 1 SE) proportion of initial carbon in (a) the detritus of *Ecklonia radiata* and *Scytothalia dorycarpa* pooled for all depths, (b) *E. radiata* detritus at each 10-, 20-, and 50-m depth, and (c) *S. dorycarpa* detritus at each 10-, 20-, and 50-m depth. Lines represent the decay models for each species and depth treatment (Table 1). Decay models for detritus at 50-m sites are omitted from the figure due to insufficient data (≥ 4 time points required to estimate negative exponential decay curves).

$p = 0.769$; Fig. 3). The initial percent nitrogen content of *S. dorycarpa* was lower than that of *E. radiata* ($t_{\text{species}[70]} = -5.899$; $p < 0.001$), and subsequently, the carbon to nitrogen (C : N) ratio was significantly higher in *S. dorycarpa* relative to *E. radiata* ($t_{\text{species}} = 4.465$; $p < 0.001$) (Supporting Information Table S6).

Export estimates (macroalgal forest to shelf break)

The particle tracking simulations from our shallow (10 and 20 m) and deep (50 m) litterbag sites show that after 2 weeks,

22.8% and 75.6% (not accounting for decomposition) of the annual flux of macroalgal POC, respectively, were exported beyond the shelf break (200 m) by local currents (Fig. 4). Within 1 month (31 d), 43.7% of particles from shallow reefs and 84.7% from deep reefs were predicted to be exported beyond the shelf break (Fig. 4). A maximum of 49.6% of particles (79 d post-release) from shallow reefs and 88.8% (90 d post release) from deep reefs were estimated to cross the shelf break, with the fate of the remaining particles remaining on the shelf and coastline. Simulated particles typically have relatively direct trajectories past the shelf edge from deep reefs but longer and more indirect trajectories from shallow reefs (Fig. 4).

We integrated decomposition rates into transport models and show that within 1 month of detritus release, an estimated 10% of *E. radiata* POC from shallow reefs (10–20 m) and 47% from deep reefs (50 m) were exported to recipient habitats exceeding 200-m depth. Similarly, 11% of *S. dorycarpa* POC from shallow reefs and 37% from the deep reefs were exported beyond the shelf break.

Discussion

Our study suggests that the decomposition rate of detritus from the Australian dominant kelp, *E. radiata*, and fucoid, *S. dorycarpa*, is similar between species. We also report similar decomposition rates at most depths (10, 20, and 50 m) within each species. The particle tracking simulation combined with our decomposition rate of particles suggests that a substantial percentage of macroalgal POC is exported beyond the shelf break (> 200 m) and into the deep ocean. Finally, our study presents the first published in situ decomposition rates for *E. radiata* and *S. dorycarpa* that can be incorporated into Australian macroalgae carbon sequestration estimates, which are substantial on a global scale.

In temperate Western Australia, half of *E. radiata* ($k = -0.06 \pm 0.03$) and *S. dorycarpa* ($k = -0.09 \pm 0.02$) detritus decomposed within 12 and 8 d, respectively. While these species decay faster than many Laminariales and Fucales in cooler regions globally (e.g., the North Pacific), regional POC export estimates from the Rottnest Continental Shelf are like or greater than global estimates due to local effects of cross-shelf currents (DSWT) and the Perth Canyon (Smith and Foreman 1984; van der Mheen et al. 2024). The majority of detritus exported past the shelf break occurs within the first month of release, approximately 11% from shallow sites and 42% from deep sites (mean between *E. radiata* and *S. dorycarpa*), which agrees well with export estimates of 17–29% for the entire shelf (when accounting for decomposition) by van der Mheen et al. (2024). Krause-Jensen and Duarte (2016) estimated that about 11% of all macroalgal detritus is sequestered as POC at the global scale, which is similar to our findings for shallow sites and lower than our POC export estimates from deep sites. We note that while Krause-Jensen and Duarte (2016) define the sequestration horizon to be 1000-m depth,

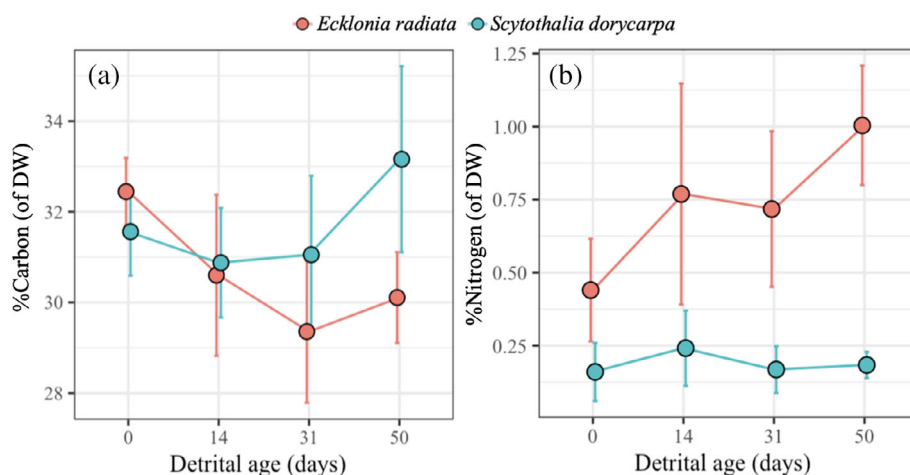


Fig. 3. Changes in (a) carbon and (b) nitrogen concentrations in macroalgae detritus over time. Mean \pm 1 SD. Sample size (n): *Ecklonia radiata*: $n_0 = 3$, $n_{14} = 49$, $n_{31} = 20$, $n_{50} = 10$; *Scytothalia dorycarpa*: $n_0 = 10$, $n_{14} = 54$, $n_{31} = 22$, $n_{50} = 11$). Data pooled for all depth treatments for each species.

sequestration timescales vary widely depending on both depth and geographic location (Siegel et al. 2021), and that recent global estimates by Filbee-Dexter et al. (2024) define the sequestration horizon to be 200 m. Off the Rottneest Continental Shelf, van der Mheen et al. (2024) suggest that there is

potentially a shallower sequestration horizon around 200 m, which we use in our study, but that may be less conservative than early global estimates.

In Western Australia, deep outer shelf reefs are projected to comprise one third of the total macroalgae reefs occurring

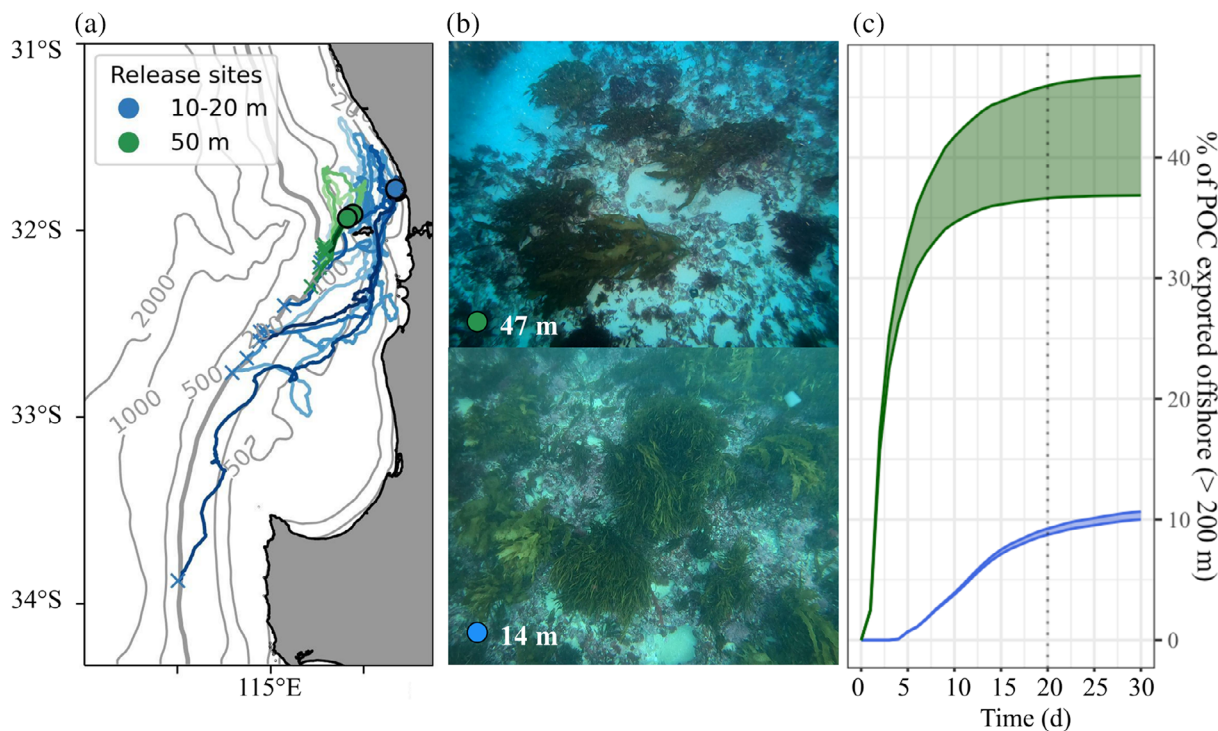


Fig. 4. Particle tracking model for detritus on the Rottneest Continental Shelf, Western Australia. (a) Map of detrital export pathways with solid circles representing particle release locations at inshore (10–20 m) and offshore (50 m) reefs. Ten random particle tracks (per each depth treatment) are shown, and crosses show the location where particles are exported below 200-m depth. (b) Photos of macroalgal forest near inshore (blue circle) and offshore (green circle) release points. (c) The percentage of particulate organic carbon (POC) (particle export accounting for decomposition) that has been exported past the continental shelf edge into the deep ocean (200 m) as a function of time (days since detritus is released). Export curves represent detritus released from in situ litterbag site coordinates at 10–20 m (blue) and 50 m (green).

between 0 and 60-m depth (Bellchambers 2017). Our particle tracking simulation estimates a shorter and more direct export pathway of POC from these outer shelf reefs to the deep ocean compared to shallow reefs. This suggests deep reefs could be important contributors to macroalgal export to the deep ocean. However, the amount of detritus produced by the deep reefs on the Rottneest Continental Shelf is unknown, and these reefs experience lower light conditions than shallow reefs, which could decrease overall productivity. Our results, therefore, cannot be used to produce a robust estimate of potential carbon sequestration of outer shelf reefs.

Based on existing *E. radiata* density for the inner Rottneest Continental Shelf (8 individuals m^{-2} on reefs) (Kendrick et al. 1999; Wernberg et al. 2003), detrital production (2 g detritus $\text{kelp}^{-1} \text{d}^{-1}$) (de Bettignies et al. 2013), and carbon content, we estimate that the detrital production averages 337 $\text{gC m}^{-2} \text{yr}^{-1}$ with mean potential carbon sequestration of 44 $\text{gC m}^{-2} \text{yr}^{-1}$ (10–20 m) during periods of cross-shelf transport (Fig. 3). Recent Australia-wide estimates for macroalgal carbon sequestration (0–30 m) suggest a rate of 35 $\text{gC m}^{-2} \text{yr}^{-1}$ (Filbee-Dexter et al. 2024). This study demonstrated that macroalgal carbon sequestration rates are similar to and potentially greater than the national estimates on coastal shallow reefs (Filbee-Dexter et al. 2024). We highlight that macroalgae that grow along coastlines that experience DSWT (or similar cross-shelf currents) could have higher than estimated potential for POC carbon export to deep ocean sinks and suggest that future studies quantify the production of macroalgae on the outer shelf to facilitate the inclusion of both shallow and deep reefs in potential carbon sequestration estimates.

We show that the decomposition of macroalgal carbon was similar between *E. radiata* and *S. dorycarpa* in 10, 20, and 50 m shelf environments, but that within *S. dorycarpa* depth treatments, decomposition in shelf environments at 20 m was significantly slower than at 10 m. The slower decomposition rate of *S. dorycarpa* at 20 m compared with 10 m might be explained by wave energy causing increased physical tissue disintegration at 10 m (Hansen 1984). We also observed at least 10 times greater biomass (FW) of colonizing invertebrates on the mid shelf vs. the inner and outer shelves (Supporting Information Table S3) and it is possible that direct consumption of decaying frond edges by amphipods at 20-m sites reduced the availability of suitable tissue for microbial colonization and subsequent decay (Singh et al. 2021). Interspecific variation in decay rate was expected between *E. radiata* and *S. dorycarpa* due to the lower percent nitrogen composition in *S. dorycarpa*. Species with high percent nitrogen and low C:N ratios typically facilitate elevated levels of microbial decay (Enriquez et al. 1993); however, we did not observe a faster decay rate in *E. radiata* compared to *S. dorycarpa*. One inherent pitfall of using litterbag experiments is that fragments smaller than the mesh size are not retained in the bags and are therefore considered remineralized when the tissue may just have been fragmented and washed out of the bags (Brouwer 1996).

Yet small mesh sizes can block light and water flow and produce unrealistic estimates of decomposition. The rapid initial decay of *S. dorycarpa* during the first 2 weeks of the experiment may have been confounded by the detachment of small reproductive receptacles (diameter = 2–4 mm) creating POC smaller than the litterbag mesh size (5 mm), potentially masking a slower decomposition rate for *S. dorycarpa*. Calculations of decay rate are therefore conservative, as fragmentation (erosion) is likely to break down tissue and result in an underestimation of percent remaining biomass.

While our study resolves macroalgal carbon sequestration potential from our litterbag experiment sites at different depths on the Rottneest Continental Shelf, there are several limitations to our estimates. Our experiment was conducted in winter when most detritus is released (de Bettignies et al. 2013); yet it is possible that higher temperatures during warmer seasons accelerate decomposition rates in summer (Filbee-Dexter et al. 2022); therefore, these rates may not represent the small amount of summer export. Despite some exceptions, within lower temperature regimes (4–10°C) (Pedersen et al. 2021), warmer temperatures usually drive faster decomposition rates of macroalgal detritus (Litchfield et al. 2020; Filbee-Dexter et al. 2022). Indeed, the mean decay rate of *E. radiata* of an ex situ litterbag experiment at 23°C ($k = -0.0629 \text{ d}^{-1}$) in New South Wales, Australia (Litchfield et al. 2020) was faster than our in situ winter experiment ($k = -0.0382 \text{ d}^{-1}$; mean temperature 20.68°C). Quantifying the effects of independent variables like light and temperature is challenging in situ and better accomplished through controlled laboratory experiments (ex situ). Future studies should test the effect of temperature and light on the breakdown of detrital carbon in ex situ experiments to understand how macroalgal POC is cycled across latitudinal and seasonal gradients.

There are also limitations to our particle tracking simulations. Although we used a high-resolution regional ocean model to force particle tracking simulations, the model does not account for dynamics < 2 km in scale. In particular, this resolution does not capture reef-scale ocean dynamics and could underestimate the retention time of simulated macroalgal detritus within a reef. We also do not account for “behavior” of macroalgal particles in our simulations, instead letting them drift passively with ocean bottom currents. Although this was justified for small and medium-sized detritus in sensitivity analyses by van der Mheen et al. (2024), the behavior of large particles of macroalgae may be different from our simulated particles. In addition, colonization by invertebrates (described above) may also change the drift behavior of detritus and potentially increase the threshold velocity at which detritus moves along the seafloor with ocean currents. Still, DSWT is the main mechanism that exports macroalgal detritus beyond the Rottneest Continental Shelf and has typical velocities of 0.15 m s^{-1} along the seafloor (van der Mheen et al. 2024), which we expect would still exceed threshold velocities of most detritus. Lastly, because these simulations

are not forced by waves or wind, we do not have the resolution to tease apart estimates of POC washed ashore and POC buried in shelf sediments (and potentially sequestered). While substantially more macroalgal carbon is expected to be sequestered through export to the deep ocean than through shelf burial (Krause-Jensen and Duarte 2016), we recommend that future simulations incorporate wave and wind forcing to estimate the percentage of POC retained on the shelf (50% of particles from shallow donor reefs) that is not washed ashore and has the potential to be sequestered in shelf sediments.

With a growing interest in macroalgal blue carbon as a mitigation strategy to climate change, it is critical to investigate regional scale carbon flows from macroalgal forests to pinpoint which areas have high carbon sequestration potential. Here we showed that carbon export potential from our experiment sites is similar for both the dominant Australian kelp, *E. radiata*, and furoid, *S. dorycarpa*, in which decomposition is relatively fast but where the presence of cross shelf currents (DSWT) can still export high percentages of POC from donor reefs. Over the course of a full year, from our 10–20 m and 50 m litterbag experiment sites, an estimated mean of 11% and 42% of macroalgal POC is transported to depths > 200 m. We suggest that future studies validate these estimates by measuring macroalgae in sediment cores from deep ocean sinks. These estimates challenge both global and Australian macroalgae blue carbon estimates, which may be underestimating carbon sequestration potential in coastal environments that experience DSWT and in outer shelf macroalgal forests that are often overlooked due to lack of offshore (> 30 m) benthic habitat surveys (Assis et al. 2018). This study supports previous modeled estimates of substantial macroalgal carbon sequestration in Australia (Krause-Jensen and Duarte 2016; Filbee-Dexter and Wernberg 2020; Filbee-Dexter et al. 2024), with estimates that include in situ decomposition rates for Australian macroalgae, and further supports the inclusion of macroalgal forests in blue carbon frameworks.

Author Contributions

Taylor Simpkins: Conceptualization; data curation; formal analysis; funding acquisition; investigation; methodology; validation; visualization; writing—original draft preparation. Karen Filbee-Dexter: Conceptualization; investigation; methodology; funding acquisition; writing—review and editing. Chari Pattiaratchi: Conceptualization; writing—review and editing. Morten F. Pedersen: Formal analysis (supporting); writing—review and editing. Albert Pessarrodona: Methodology; writing—review and editing. Mirjam Van Der Mheen: Methods; investigation; visualization (supporting); writing—original draft preparation. Thomas Wernberg: Conceptualization; funding acquisition; writing—review and editing.

Acknowledgments

This work was funded by an OceanWorks Prototyping Grant (to Taylor Simpkins) and the Australian Research

Council (DP220100650 and LP220100004 to Thomas Wernberg and Karen Filbee-Dexter and FT230100214 to Karen Filbee-Dexter). We acknowledge the contribution of Randall Simpkins for mooring design; Jurgen Valckenaere, Mason Sullivan, Celina Burkholz, Samuel Rose, Defne Singh, and Jessica Walker for their assistance in the field; Megan Proctor and Antoine Minne for their support with sample preparation; and Luka Wright for his expertise in nls modeling (RStudio). Open access publishing facilitated by The University of Western Australia, as part of the Wiley - The University of Western Australia agreement via the Council of Australian University Librarians.

Conflict of Interest

There are no conflicts of interest.

References

- Assis, J., E. Á. Serrão, N. C. Coelho, F. Tempera, M. Valero, and F. Alberto. 2018. “Past Climate Changes and Strong Oceanographic Barriers Structured Low-Latitude Genetic Relics for the Golden Kelp *Laminaria ochroleuca*.” *Journal of Biogeography* 45: 2326–2336. <https://doi.org/10.1111/jbi.13425>.
- Banta, G. T., M. F. Pedersen, and S. L. Nielsen. 2004. “Decomposition of Marine Primary Producers: Consequences for Nutrient Recycling and Retention in Coastal Ecosystems.” In *Estuarine Nutrient Cycling: The Influence of Primary Producers: The Fate of Nutrients and Biomass*, edited by G. T. Banta, M. F. Pedersen, and S. L. Nielsen, 187–216. Kluwer Academic Publishers. <https://forskning.ruc.dk/en/publications/decomposition-of-marine-primary-producers-consequences-for-nutrie>.
- Bedford, A. P., and P. G. Moore. 1984. “Macrofaunal Involvement in the Sublittoral Decay of Kelp Debris: The Detritivore Community and Species Interactions.” *Estuarine, Coastal and Shelf Science* 18: 97–111. [https://doi.org/10.1016/0272-7714\(84\)90009-X](https://doi.org/10.1016/0272-7714(84)90009-X).
- Bellchambers, L. M., J. How, S. N. Evans, M. B. Peber, S. de Lestang and N. Caputi. 2017. Ecological Assessment Report: Western Rock Lobster Resource of Western Australia Fisheries Research Report No. 279, Department of Fisheries, Western Australia. 92pp.
- Bertram, C., M. Quaas, T. B. H. Reusch, A. T. Vafeidis, C. Wolff, and W. Rickels. 2021. “The Blue Carbon Wealth of Nations.” *Nature Climate Change* 11: 704–709. <https://doi.org/10.1038/s41558-021-01089-4>.
- Broch, O. J., K. Hancke, and I. H. Ellingsen. 2022. “Dispersal and Deposition of Detritus From Kelp Cultivation.” *Frontiers in Marine Science* 9: 840531. <https://doi.org/10.3389/fmars.2022.840531>.
- Brouwer, P. E. M. 1996. “Decomposition In Situ of the Sublittoral Antarctic Macroalga *Desmarestia anceps* Montagne.”

- Polar Biology* 16: 129–137. <https://doi.org/10.1007/BF02390433>.
- Coleman, M. A., and T. Wernberg. 2017. “Forgotten Underwater Forests: The Key Role of Fucoids on Australian Temperate Reefs.” *Ecology and Evolution* 7: 8406–8418. <https://doi.org/10.1002/ece3.3279>.
- Dagestad, K.-F., J. Röhrs, Å. y. Breivik, and B. Ådlandsvik. 2018. “OpenDrift v1.0: A Generic Framework for Trajectory Modelling.” *Geoscientific Model Development* 11: 1405–1420. <https://doi.org/10.5194/gmd-11-1405-2018>.
- de Bettignies, F., P. Dauby, F. Thomas, et al. 2020. “Degradation Dynamics and Processes Associated with the Accumulation of *Laminaria hyperborea* (Phaeophyceae) Kelp Fragments: An In Situ Experimental Approach.” *Journal of Phycology* 56: 1481–1492. <https://doi.org/10.1111/jpy.13041>.
- de Bettignies, T., T. Wernberg, P. S. Lavery, M. A. Vanderklift, and M. B. Mohring. 2013. “Contrasting Mechanisms of Dislodgement and Erosion Contribute to Production of Kelp Detritus.” *Limnology and Oceanography* 58: 1680–1688. <https://doi.org/10.4319/lo.2013.58.5.1680>.
- Enriquez, S., C. M. Duarte, and K. Sand-Jensen. 1993. “Patterns in Decomposition Rates among Photosynthetic Organisms: The Importance of Detritus C:N:P Content.” *Oecologia* 94: 457–471. <https://doi.org/10.1007/BF00566960>.
- Filbee-Dexter, K., and T. Wernberg. 2020. “Substantial Blue Carbon in Overlooked Australian Kelp Forests.” *Scientific Reports* 10: 12341.
- Filbee-Dexter, K., M. F. Pedersen, S. Fredriksen, et al. 2020. “Carbon Export Is Facilitated by Sea Urchins Transforming Kelp Detritus.” *Oecologia* 192: 213–225. <https://doi.org/10.1007/s00442-019-04571-1>.
- Filbee-Dexter, K., C. J. Feehan, A. S. Dan, et al. 2022. “Kelp Carbon Sink Potential Decreases With Warming Due to Accelerating Decomposition.” *PLoS Biology* 20: e3001702. <https://doi.org/10.1371/journal.pbio.3001702>.
- Filbee-Dexter, K., M. F. Pedersen, S. Fredriksen, et al. 2024. “Carbon Export from Seaweed Forests to Deep Ocean Sinks.” *Nature Geoscience* 17: 552–559. <https://doi.org/10.1038/s41561-024-01449-7>.
- Frontier, N., F. de Bettignies, A. Foggo, and D. Davoult. 2021. “Sustained Productivity and Respiration of Degrading Kelp Detritus in the Shallow Benthos: Detached or Broken, but Not Dead.” *Marine Environmental Research* 166: 105277. <https://doi.org/10.1016/j.marenvres.2021.105277>.
- Hansen, J. 1984. “Accumulations of Macrophyte Wrack along Sandy Beaches in Western Australia: Biomass, Decomposition Rates and Significance in Supporting Nearshore Production.” PhD thesis, The University of Western Australia.
- Hurd, C. L., C. S. Law, L. T. Bach et al. 2022. “Forensic Carbon Accounting: Assessing the Role of Seaweeds for Carbon Sequestration.” *Journal of Phycology* 58: 347–363. <https://doi.org/10.1111/jpy.13249>.
- Ivanov, V. V., G. I. Shapiro, J. M. Huthnance, D. L. Aleynik, and P. N. Golovin. 2004. “Cascades of Dense Water around the World Ocean.” *Progress in Oceanography* 60: 47–98. <https://doi.org/10.1016/j.pocean.2003.12.002>.
- Kendrick, G. A., P. S. Lavery, and J. C. Phillips. 1999. “Influence of *Ecklonia radiata* Kelp Canopy on Structure of Macro-Algal Assemblages in Marmion Lagoon, Western Australia.” *Hydrobiologia* 398–399: 275–283. <https://doi.org/10.1023/A:1017011124938>.
- Kirschbaum, M. U. F. 2010. “The Temperature Dependence of Organic Matter Decomposition: Seasonal Temperature Variations Turn a Sharp Short-Term Temperature Response Into a More Moderate Annually Averaged Response: Temperature Dependence of Organic Matter Decomposition.” *Global Change Biology* 16: 2117–2129. <https://doi.org/10.1111/j.1365-2486.2009.02093.x>.
- Krause-Jensen, D., and C. M. Duarte. 2016. “Substantial Role of Macroalgae in Marine Carbon Sequestration.” *Nature Geoscience* 9: 737–742. <https://doi.org/10.1038/ngeo2790>.
- Kristensen, E. 1994. “Decomposition of Macroalgae, Vascular Plants and Sediment Detritus in Seawater; Use of Stepwise Thermogravimetry.” *Biogeochemistry* 26: 1–24. <https://doi.org/10.1007/BF02180401>.
- Krumhansl, K. A., and R. E. Scheibling. 2012. “Production and Fate of Kelp Detritus.” *Marine Ecology. Progress Series* 467: 281–302. <https://doi.org/10.3354/meps09940>.
- Litchfield, S. G., K. G. Schulz, and B. P. Kelaher. 2020. “The Influence of Plastic Pollution and Ocean Change on Detrital Decomposition.” *Marine Pollution Bulletin* 158: 111354. <https://doi.org/10.1016/j.marpolbul.2020.111354>.
- Macreadie, P. I., M. D. P. Costa, T. B. Atwood, et al. 2021. “Blue Carbon as a Natural Climate Solution.” *Nature Reviews Earth and Environment* 2: 826–839. <https://doi.org/10.1038/s43017-021-00224-1>.
- Macreadie, P. I., A. Anton, J. A. Raven, et al. 2019. “The Future of Blue Carbon Science.” *Nature Communications* 10: 3913–3998. <https://doi.org/10.1038/s41467-019-11693-w>.
- Mahjabin, T., C. Pattiaratchi, and Y. Hetzel. 2020. “Occurrence and Seasonal Variability of Dense Shelf Water Cascades along Australian Continental Shelves.” *Scientific Reports* 10: 9732. <https://doi.org/10.1038/s41598-020-66711-5>.
- Mahjabin, T., C. Pattiaratchi, Y. Hetzel, and I. Janekovic. 2019. “Spatial and Temporal Variability of Dense Shelf Water Cascades along the Rottneest Continental Shelf in Southwest Australia.” *Journal of Marine Science and Engineering* 7: 30. <https://doi.org/10.3390/jmse7020030>.
- Martinez, B., B. Radford, S. Thomsen, et al. 2018. “Distribution Models Predict Large Contractions of Habitat-Forming Seaweeds in Response to Ocean Warming.” *Diversity and Distributions* 24: 1350–1366. <https://doi.org/10.1111/ddi.12767>.
- Ortega, A., N. R. Galdi, I. Alam, et al. 2019. “Important Contribution of Macroalgae to Oceanic Carbon Sequestration.” *Nature Geoscience* 12: 748–754. <https://doi.org/10.1038/s41561-019-0421-8>.

- Paine, E. R., M. Schmid, P. W. Boyd, G. Diaz-Pulido, C. L. Hurd, and C. Pfister. 2021. "Rate and Fate of Dissolved Organic Carbon Release by Seaweeds: A Missing Link in the Coastal Ocean Carbon Cycle." *Journal of Phycology* 57: 1375–1391. <https://doi.org/10.1111/jpy.13198>.
- Pattiaratchi, C., B. Hollings, M. Woo, and T. Welhena. 2011. "Dense Shelf Water Formation Along the South-West Australian Inner Shelf." *Geophysical Research Letters* 38: L10609. <https://doi.org/10.1029/2011GL046816>.
- Pedersen, M. F., K. Filbee-Dexter, N. L. Frisk, Z. Sarossy, and T. Wernberg. 2021. "Carbon Sequestration Potential Increased by Incomplete Anaerobic Decomposition of Kelp Detritus." *Marine Ecology. Progress Series* 660: 53–67. <https://doi.org/10.3354/meps13613>.
- Pedersen, M. F., and K. L. Johnsen. 2017. "Nutrient (N and P) Dynamics of the Invasive Macroalga *Gracilaria vermiculophylla*: Nutrient Uptake Kinetics and Nutrient Release through Decomposition." *Marine Biology* 164: 1. <https://doi.org/10.1007/s00227-017-3197-7>.
- Pedersen, M. F., K. Filbee-Dexter, K. M. Norderhaug, et al. 2019. "Detrital Carbon Production and Export in High Latitude Kelp Forests." *Oecologia* 192: 227–239. <https://doi.org/10.1007/s00442-019-04573-z>.
- Pessarrodona, A., K. Filbee-Dexter, K. A. Krumhansl, M. F. Pedersen, P. J. Moore, and T. Wernberg. 2022. "A Global Dataset of Seaweed Net Primary Productivity." *Scientific Data* 9: 484. <https://doi.org/10.1038/s41597-022-01554-5>.
- Pessarrodona, A., R. M. Franco-Santos, L. S. Wright, et al. 2023. "Carbon Sequestration and Climate Change Mitigation Using Macroalgae: A State of Knowledge Review." *Biological Reviews of the Cambridge Philosophical Society*. <https://doi.org/10.1111/brv.12990>.
- Pidgeon, E. 2021. Blue Carbon: Integrating Ocean Ecosystems in Global Climate Action. Conservation International. <https://www.conservation.org/docs/default-source/publication-pdfs/blue-carbon-integrating-ocean-ecosystems-october-2021a.pdf>.
- Queiros, A. M., K. Tait, J. R. Clark, et al. 2023. "Identifying and Protecting Macroalgae Detritus Sinks toward Climate Change Mitigation." *Ecological Applications* 33: e2798. <https://doi.org/10.1002/eap.2798>.
- Robertson, A. I., and J. S. Lucas. 1983. "Food Choice, Feeding Rates, and the Turnover of Macrophyte Biomass by a Surf-Zone Inhabiting Amphipod." *Journal of Experimental Marine Biology and Ecology* 72: 99–124. [https://doi.org/10.1016/0022-0981\(83\)90138-7](https://doi.org/10.1016/0022-0981(83)90138-7).
- Siegel, D. A., T. DeVries, S. C. Doney, and T. Bell. 2021. "Assessing the Sequestration Time Scales of Some Ocean-Based Carbon Dioxide Reduction Strategies." *Environmental Research Letters* 16: 104003. <https://doi.org/10.1088/1748-9326/ac0be0>.
- Singh, C. L., M. J. Huggett, P. S. Lavery, C. Sawstrom, and G. A. Hyndes. 2021. "Kelp-Associated Microbes Facilitate Spatial Subsidy in a Detrital-Based Food Web in a Shoreline Ecosystem." *Frontiers in Marine Science* 8: 678222. <https://doi.org/10.3389/fmars.2021.678222>.
- Skrzypek, G. 2013. "Normalization Procedures and Reference Material Selection in Stable HCNOS Isotope Analyses: An Overview." *Analytical and Bioanalytical Chemistry* 405: 2815–2823. <https://doi.org/10.1007/s00216-012-6517-2>.
- Smith, B. D., and R. E. Foreman. 1984. "An Assessment of Seaweed Decomposition within a Southern Strait of Georgia Seaweed Community." *Marine Biology* 84: 197–205. <https://doi.org/10.1007/BF00393005>.
- Stephen, L. 2021. "IPCC, 2021: Climate Change 2021—The Physical Science Basis." *Interactions* 49: 44–45.
- Trevathan-Tackett, S. M., J. Kelleway, P. I. Macreadie, J. Beardall, P. Ralph, and A. Bellgrove. 2015. "Comparison of Marine Macrophytes for their Contributions to Blue Carbon Sequestration." *Ecology* 96: 3043–3057. <https://doi.org/10.1890/15-0149.1>.
- van der Mheen, M., T. Wernberg, C. Pattiaratchi, et al. 2024. "Substantial Kelp Detritus Exported Beyond the Continental Shelf by Dense Shelf Water Transport." *Scientific Reports* 14: 839. <https://doi.org/10.1038/s41598-023-51003-5>.
- Vanderklift, M. A., D. Herr, C. E. Lovelock, D. Murdiyarso, J. L. Raw, and A. D. L. Steven. 2022. "A Guide to International Climate Mitigation Policy and Finance Frameworks Relevant to the Protection and Restoration of Blue Carbon Ecosystems." *Frontiers in Marine Science* 9: 872064. <https://doi.org/10.3389/fmars.2022.872064>.
- Vetter, E. W., and P. K. Dayton. 1998. "Macrofaunal Communities Within and Adjacent to a Detritus-Rich Submarine Canyon System." *Deep-Sea Research Part II: Topical Studies in Oceanography* 45: 25–54. [https://doi.org/10.1016/S0967-0645\(97\)00048-9](https://doi.org/10.1016/S0967-0645(97)00048-9).
- Wernberg, T. 2019. "Biology and Ecology of the Globally Significant Kelp *Ecklonia radiata*." *Oceanography and Marine Biology* 57: 265–324. <https://doi.org/10.1201/9780429026379-6>.
- Wernberg, T., G. A. Kendrick, and J. C. Phillips. 2003. "Regional Differences in Kelp-Associated Algal Assemblages on Temperate Limestone Reefs in South-Western Australia." *Diversity and Distributions* 9: 427–441. <https://doi.org/10.1046/j.1472-4642.2003.00048.x>.
- Wolff, T. 1962. The Systematics and Biology of Bathyal and Abyssal Isopoda Asellota. Galathea Reports. Copenhagen: Zoological Museum.
- Wolter, K., and M. S. Timlin. 2011. "El Niño/Southern Oscillation Behaviour Since 1871 as Diagnosed in an Extended Multivariate ENSO Index (MEI.ext): El Niño/Southern Oscillation Behaviour Since 1871." *International Journal of Climatology* 31: 1074–1087. <https://doi.org/10.1002/joc.2336>.
- Wormersley, H. B. S. 1987. The Marine Benthic Flora of Southern Australia. Part II. Adelaide, South Australia: South Australian Government Printing Division.
- Wright, L. S., A. Pessarrodona, and A. Foggo. 2022. "Climate-Driven Shifts in Kelp Forest Composition Reduce Carbon Sequestration Potential." *Global Change Biology* 28: 5514–5531. <https://doi.org/10.1111/gcb.16299>.

- Yamagata, T., N. H. Saji, B. N. Goswami, and P. N. Vinayachandran. 1999. "A Dipole Mode in the Tropical Indian Ocean." *Nature (London)* 401: 360–363. <https://doi.org/10.1038/43854>.
- Zarco-Perello, S., T. J. Langlois, T. Holmes, M. A. Vanderklift, and T. Wernberg. 2019. "Overwintering Tropical Herbivores Accelerate Detritus Production on Temperate Reefs." *Proceedings of the Royal Society B: Biological Sciences* 286: 20192046. <https://doi.org/10.1098/rspb.2019.2046>.

Supporting Information

Additional Supporting Information may be found in the online version of this article.

Submitted 01 October 2023

Revised 29 March 2024

Accepted 01 February 2025